Compatibilities and Electrostatic Interactions in the Blends of Self-Acid-Doped Conjugated Conducting Polymer, Poly[2-(3′-thienyl)ethanesulfonic acid], and Its Sodium Salt with Poly(vinyl alcohol)

Show-An Chen* and Mu-Yi Hua

Chemical Engineering Department, National Tsing-Hua University, Hsinchu, Taiwan 30043, R.O.C.

Received September 28, 1995; Revised Manuscript Received April 18, 1996[⊗]

ABSTRACT: The structure and properties of the blends poly[sodium 2-(3′-thienyl)ethanesulfonate] (P3TESNa)/poly(vinyl alcohol) (PVA) and poly[2-(3′-thienyl)ethanesulfonic acid] (P3TESH)/PVA, both with a mole ratio 1/1 of the two components, were investigated by gel permeation chromatography (GPC), X-ray diffraction (XRD), infrared spectroscopy (IR), ultraviolet−visible−near-infrared spectroscopy (UV−vis−near-IR), X-ray photoelectron spectroscopy (XPS), dynamic mechanical analysis (DMA), and conductivity. The blends were cast from water solutions of the two components. The P3TESH/PVA blend consists of the two phases, a P3TESH phase and a P3TESH/PVA complex phase, in which no characteristic of the PVA component is observed. In the complex phase, the two polymers are intimately mixed. However, this compatibility is different from that of conventional polymer blends in that the present blend has an additional phase composed of one of the two pure components. The phase with the complexes has glass transition and side chain relaxation temperatures higher than that of the pure components, and has new chain packing as reflected in a new X-ray diffraction peak (2θ) at 21.5°. This type of compatibility results from the hydrogen-bonding (or electrostatic) interaction between the two components and the strong aggregation of one component (in this case, P3TESH). The blending of P3TESH with PVA leads to a significant undoping, and the conductivity decreases from 10^{-2} S/cm in the pure state to 10^{-6} S/cm. The P3TESH subchains that are not self-acid-doped (or containing the $-SO_3H$ group) exhibit a red shift of the UV−vis absorption maximum by 44 nm, resulting from an increase in coplanarity caused by a repulsion between neighboring $-SO_3-$ groups. For the P3TESNa/PVA blend, the phase structure and electrostatic interaction are similar to those in the above blend. A drastic red shift of the UV−vis absorption maximum by 76 nm (0.52 eV) accompanied by a color change from pale orange-yellow to bright orange-red after the blending is observed. The red shift results from the strong electrostatic interaction between the Na^+ ion of P3TESNa and the O atom of PVA. Such a large red shift is equivalent to the thermochromism and solvatochromism of poly(3-alkylthiophene)s. The conductivity of P3TESNa (10^{-7} S/cm) drops by 1 order of magnitude after blending with PVA, but the blend can be doped by a protonic acid to give a conductivity of 10^{-3} S/cm.

Introduction

Conjugated polymers can be doped chemically or electrochemically by oxidization or reduction accompanied by an insertion of dopant ions, which can be either located externally or bound to the polymer chains. The latter type of doping is termed "self-doping" or, when the dopant is an acid, as "self-acid-doping" such as in poly[*n*-(3′-thienyl)alkanesulfonic acid] (P3TASH)[1,2] **(I)**, sulfonic acid ring-substituted polyaniline,[3]

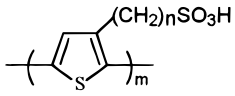

n = 2, 6, and 10

(I)

and poly(aniline-*co*-*N*-propanesulfonic acid−aniline).[4] The self-acid-doped conducting polymer is different from the self-doped conducting polymer prepared by the electrochemical method, which produces "ejection" of π-electrons on the main chains and protons (or cations) on the side chains. The detailed structure of P3TASH consists of four basic units: the neutral unit (structure **I**), polaron, bipolaron, and the unit having the thiophene ring with an sp^3 α-carbon and positive charge resulting from the proton addition, as reported in our previous paper.[2] P3TASH has been found to have potential applications in display technologies owing to its fast response in electrochemical chromism[5] and in electron beam lithography owing to its conductivity and water solubility.[6] Since P3TASH and P3TESNa are brittle and can absorb large amounts of moisture, it is sometimes desirable to improve these shortcomings by blending with conventional water soluble polymers.

Since conjugated conducting polymers without long flexible side chains are brittle, particularly after doping, blending with conventional polymers in order to improve their mechanical properties and processability and to reduce the cost has been attempted. The poly(3-hexylthienylene-*co*-3-benzylthienylene)/polystyrene (PS) blend (weight ratio 1/2) was found to be incompatible since the electronic absorption spectra of the former component remain the same before and after the blending.[7] The poly(3-octylthiophene)/polystyrene blend (weight ratio 82/18) was also found to be incompatible.[8] The blends of polypyrrole (PPy) with PS and with polycarbonate (PC) are both incompatible, but PPy interacts more strongly with PC than with PS, due to hydrogen bonding as found by infrared spectroscopy (IR) and SEM.[9] Polyaniline (PAn)/poly(vinyl alcohol) (PVA) blends prepared electrochemically are incompatible and have a PAn gradient along the film thickness, in which some PVA subchains were grafted by PAn chains.[10] In the presence of polymeric acid as a template for oxidative polymerization of aniline, the reaction product was

[⊗] Abstract published in *Advance ACS Abstracts,* June 1, 1996.

S0024-9297(95)01460-4 CCC: $12.00

found to be water soluble;[11,12] however, microstructures of this blend were not reported. The poly(amic acid)/PAn blend and its cured product, the polyimide/PAn blend, were claimed to be miscible on a molecular scale since the cured poly(amic acid) lost its wide angle X-ray scattering (WAXS) reflection peak at $2\theta = 5.9°$ in the blend.[13] In a poly(acrylic acid) (PAA)/PAn blend (mole ratio of their repeat units, 1/1) obtained by casting from NMP, a two-phase-structure consisting of a PAA-doped PAn phase and an undoped PAn phase both with a domain size of about 0.05 μm was observed using atomic force microscopy.[14] The blend of PAn with poly(vinylpyrrolidone), which acts as a hydrogen bond acceptor with PAn, was claimed to be either miscible based on thermal and dynamic mechanical analyses or phase-separated with a small domain size of 500−1000 Å based on small angle X-ray scattering and optical microscopy.[15]

This work reports studies of spectroscopic and thermal analyses on the blends of P3TESH and its sodium salt with poly(vinyl alcohol). It is found that contrary to other conjugated polymer blends reviewed above, P3TESH interacts strongly with PVA through hydrogen bonding. So that, in the blend, no crystalline and amorphous characteristics of PVA and no amorphous characteristic of P3TESH were observed and that a new phase of P3TESH/PVA complex, in addition to the ordered P3TESH phase, is formed. Similar results for the blend of P3TESNa with PVA were also obtained, and a drastic red shift by 76 nm equivalent to those in thermochromism and solvatochromism of poly(3-alkylthiophene)s was observed, resulting from a strong electrostatic interaction.

Experimental Section

1. Synthesis of Polymers and Preparation of Samples. The monomer, sodium 2-(3′-thienyl)ethanesulfonate (3-TESNa), was prepared and purified as proposed by Ikenoue and co-workers[1] and was characterized by use of ^{1}H NMR to assure that the side chain was on the 3-position of the rings. Neutral poly[sodium 2-(3′-thienyl)ethanesulfonate] (P3TESNa) was prepared by following the chemical method used by Sugimoto et al.[16] and Ikenoue and co-workers.[1] 3-TESNa (0.1 N) was oxidatively polymerized in a 0.4 N $FeCl_3$ solution in H_2O at room temperature under a nitrogen atmosphere.[1,2] The water in the resulting mixture was removed in a rotatory evaporator under vacuum at 50 °C and washed several times with absolute ethanol. The polymer formed was extracted with absolute ethanol in a Soxhlet extractor in order to remove the residual oxidant and oligomers. The purified polymer (P3TESNa) was dried to constant weight under continuous vacuum pumping at room temperature. The P3TESNa was then converted to poly[2-(3′-thienyl)ethanesulfonic acid] (P3TESH) by mixing an aqueous solution of P3TESNa with an H^+-type ion exchange resin in a rotating bottle for 6 h. The resin used for exchanging Na^+ with H^+ was a Rohm and Haas IR 120H (H^+-type) resin having the diameter 0.3−1.2 mm. The polymer so obtained, P3TESH, was dried under continuous vacuum pumping at room temperature to constant weight.

Blends of P3TESNa/PVA and P3TESH/PVA, 1/1 ratio of the repeat units, were prepared by mixing in water, according to the following procedure. First, PVA was fully dissolved in water at 80 °C, cooled to room temperature, added to P3TESNa or P3TESH aqueous solutions, and stirred until the solutions were homogeneous. Most of the water was then removed in a rotatory evaporator under vacuum at room temperature. The concentrated solution was cast in a Teflon mold to give thin films (about 0.1 mm), which were subjected to continuous vacuum pumping to remove residual water until constant weights were reached.

For the preparation of PVA films, the fully dissolved PVA aqueous solution was cooled from 80 °C to room temperature, concentrated, and dried using the same procedure for the blends.

2. Characterizations. Gel permeation chromatography (Waters Model 201) with a UV detector at 431 nm for P3TESNa, 415 nm for P3TESH, and 190 nm for PVA and a column of TSKgel GMPWXL from Tosoh was used to measure to molecular weight distribution (MWD) relative to poly(vinyl alcohol) and poly(acrylic acid) standards at room temperature. The calibration curve was determined by use of six MW standards from MW 1250 to 7.5×10^5. The carrier solvent used was degassed and deionized water at a flow rate of 0.4 mL/min.

X-ray diffractions (XRD) were measured using a Rigaku Model D/Max-2B diffractometer at room temperature. The X-ray beam was nickel-filtered Cu Kα ($\lambda = 1.54$ Å) radiation from a sealed tube operated at 30 kV and 20 mA. The source and receiving slit widths were each 1°. Diffraction intensity data were obtained from 5 to 30° (2θ) at a scan rate of 1°/min with a smoothing number of 7.

Infrared spectra (IR) of the polymers were recorded using a Perkin-Elmer Model 983 infrared spectrophotometer at a resolution of 3 cm^{-1} and reported in wavenumbers (ν, cm^{-1}). The samples were prepared by grinding the polymers in powder form with KBr powder and then compressing into pellets.

Ultraviolet−visible−near-IR spectra (UV−vis−near-IR) of polymer films coated on glass plates were recorded using a UV−vis−near-IR spectrometer (Perkin-Elmer UV−vis−near-IR spectrometer, Lambda 19).

X-ray photoelectron spectroscopy (XPS) measurements were made on a Perkin-Elmer Model 1905 XPS spectrometer with a twin-anode X-ray gun (Mg Kα and Al Kα lines at 1253.6 and 1486.6 eV photons, respectively). High-resolution scans were obtained with the magnesium source operating at 12 kV and 250 W. All measurements were made with take off angle of 60° and a pass energy of 25 eV. The pressure in the analysis chamber was maintained at 10^{-8} Torr or lower during the measurements. The binding energies were referenced to the hydrocarbon component in the C(1s) envelope, defined to be 285.0 eV to compensate for surface charging. In spectral deconvolution, the line widths (full width at half-maximum) of Gaussian peaks were kept constant for all components in a specific spectrum.[17] Surface elemental stoichiometries were determined from peak area ratios with an error of about ±7%.

Dynamic mechanical analysis (DMA, DuPont Model DMA 983) was used to measure the dynamic flexural modulus (E' and E'') of the polymer films in the temperature range −100 to +230 °C at a heating rate of 2 °C/min and a frequency of 1 Hz. The sample size was about 10 mm long, 2 mm wide, and 0.1 mm thick. After mounting a specimen in the sample chamber, the sample length subject to cyclic flexural motion was about 1 mm. During the measurement, each sample except P3TESH in the sample cell was subjected to moisture removal by heat scanning from room temperature to 100 °C and then cooling to 50 °C . For P3TESH, in order to prevent the sample from thermal undoping at 100 °C, the sample was subjected to dynamic vacuum pumping at 38 °C for 2 weeks to remove the moisture first and then immediately transferred to the sample cell.

Conductivities of P3TESNa, P3TESH, and the blends P3TESNa/PVA and P3TESH/PVA were measured using the four probe method[18] at room temperature under dry nitrogen gas purging at a flow rate of 40 mL/min.

Results and Discussion

1. Gel Permeation Chromatography (GPC) Results. The number- and weight-average molecular weights, $\bar{M}_n$ and $\bar{M}_w$, and average degree of polymerization $\overline{DP}_n$ (relative to the molecular weight standards of poly(vinyl alcohol) and poly(acrylic acid)) of P3TESNa, P3TESH, and PVA so obtained are listed in Table 1. The $\bar{M}_w$ of P3TESNa, P3TESH and PVA are of the order of 10^5, which is sufficient to consider them high polymers. Although P3TESH was converted from P3TESNa

Table 1. Average Molecular Weights of P3TESNa, P3TESH, and PVA Relative to Poly(vinyl alcohol) and Poly(acrylic acid) Standards[a]

	$\bar{M}_n$, 10^{-5}	$\bar{M}_w$, 10^{-5}	$\bar{M}_w/\bar{M}_n$	$\overline{DP}_n$
P3TESNa	2.92	3.27	1.12	1542
P3TESH	5.80	7.06	1.22	3714
PVA	0.82	1.92	2.34	4371

[a] The molecular weights were determined from the molecular weight distribution curve. The calibration curve used was obtained by employing the linear regression ($M_i = D_0 + D_1 t_i + D_2 t_i^2 + D_3 t_i^3$) on six molecular weight standards, where M_i and t_i are molecular weight and elution time of count i and D's are coefficients.

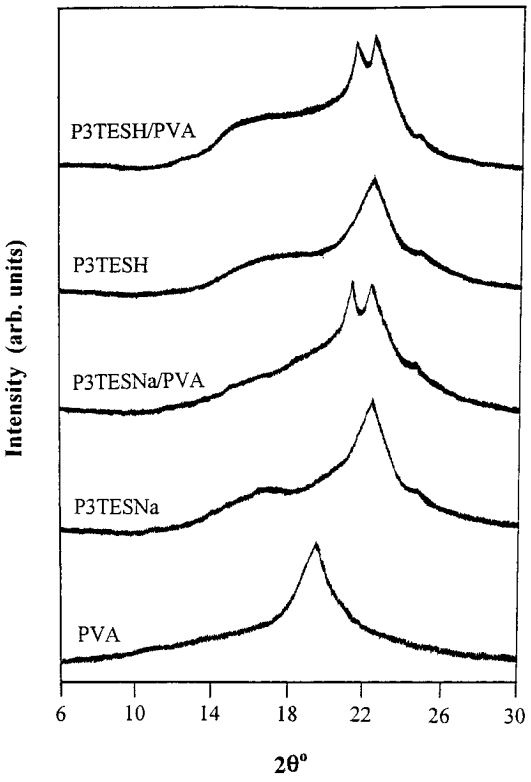

Figure 1. X-ray diffraction patterns of PVA, P3TESNa, P3TESH, and the blends P3TESNa/PVA and P3TESH/PVA at room temperature.

via ion exchange the $\overline{DP}_n$ of P3TESH is about twice that of P3TESNa, probably because intermolecular aggregation is higher in P3TESH.

2. X-ray Diffraction. X-ray diffraction patterns of PVA, P3TESNa, P3TESH, and the blends of P3TESNa/PVA and P3TESH/PVA both with a 1/1 ratio of repeat units are shown in Figure 1; their characteristic angles at intensity maxima and corresponding values of d spacing calculated using the Bragg's law are listed in Table 2. For PVA, a broad diffused scattering peak ranging from $2\theta = 9$ to 28° with a moderate intensity peak at $2\theta = 19.5°$ ($d = 4.6$ Å) is observed, indicating the coexistence of disorder and crystalline phases[19] in the bulk polymer. The X-ray diffraction patterns of P3TESNa and P3TESH are nearly the same; each has a peak with moderate intensity centered at $2\theta = 22.5°$ ($d = 4.0$ Å) and a broad peak centered at $2\theta = 16°$ ($d = 5.5$ Å). The former peak can be attributed to disorder and short-range order phases, and the latter peak, to the interplanar spacing with a broad distribution resulting from the $-C_2H_4SO_3Na$ or $-C_2H_4SO_3H$ side groups. Moreover, the d spacing 4.0 Å of the short-range order phases of P3TESNa and P3TESH can be attributed to the spacing between two successive stacking planes of coplanar subchains (or intralayer spacing), as was also assigned for P3ATs.[20,21]

Table 2. X-ray Diffraction Maxima and Calculated *d* Spacing of PVA, P3TESNa, P3TESH, and the Blends P3TESNa/PVA and P3TESH/PVA

	2θ, deg/d spacing, Å	
sample	small angle	wide angle
PVA		19.5/4.6
P3TESNa	16/5.5	22.5/4.0
P3TESH	16.5/5.4	22.4/4.0
P3TESNa/PVA blend[a]	13/6.8−20.8/4.3	21.5/4.1
		22.5/4.0
P3TESH/PVA blend[a]	16.5/5.4	21.2/4.2
		22.4/4.0

[a] Mole ratio of the repeat units = 1/1.

For the P3TESNa/PVA and P3TESH/PVA blends, the original diffraction peaks of P3TESNa and P3TESH at the wide angle 2θ of about 22.5° still appear, while that of PVA disappears; but a new diffraction peak generates at $2\theta = 21.5°$ ($d = 4.1$ Å). The original weak dispersive peak of P3TESNa and P3TESH in the range $2\theta = 13-20°$ becomes weaker for the blend with P3TESNa but stronger for the blend with P3TESH. This difference could be due to the bulkiness of Na^+ which can prevent the side chain from ordered alignment. These results indicate that, in the blends, parts of the original order phases of P3TESNa and P3TESH are still preserved, but new short-range order phases composed of strongly interacted P3TESNa/PVA and P3TESH/PVA complexes are formed.

3. Infrared Spectroscopy (IR). IR spectra of PVA, P3TESNa, P3TESH, and the blends of P3TESNa/PVA and P3TESH/PVA are shown in Figure 2. For PVA, the characteristic absorption peaks[22] are 3443 (O—H stretching), 2927 (saturated C—H stretching), 1451 (O—H and C—H bending), 1381 (C—H in-plane bending), 1333 (C—H and O—H bending), 1262 (C—H wagging), 1141 (crystallization-sensitive band),[23] and 1095 cm^{-1} (C—H stretching and O—H bending). The absorption at 1141 cm^{-1} indicates a crystalline phase in PVA,[23] in agreement with the XRD observation above. For P3TESNa, the characteristic absorption peaks[2,24,25] are 2931 (saturated C—H stretching), 1466 and 1415 (thiophene ring stretching), 1370 (C—H in-plane bending), 1312 (C—H wagging), 1182 (asymmetric $S(=O)_2$ stretching), 1049 (symmetric $S(=O)_2$ stretching), and 808 cm^{-1} (C_β—H out-of plane bending). For P3TESH, the characteristic absorption peaks[2,24,25] are 1308 (T_4 mode, C=C stretching), 1169 and 1104 (including T_2 and T_3 (C-C stretching), C_β—H in-plane bending, asymmetric $S(=O)_2$ stretching, and O—H bending), 1041 (symmetric $S(=O)_2$ stretching), and 969 cm^{-1} (T_1 mode). These T (transition) modes are related to the translational motion of intrinsic charged defects (polarons and bipolarons) arising from the electron−phonon interactions.[24,25]

A comparison of the spectrum for the blend P3TESNa/PVA (Figure 2) with the spectra of pure components PVA and P3TESNa shows that the absorption peaks of O—H stretching at 3443 cm^{-1} and O—H bending at 1451 cm^{-1} of the blend shift by 8 and 12 cm^{-1} to the lower wavenumbers 3435 and 1439 cm^{-1}, respectively. This indicates an electrostatic interaction between the two components. Because the basicity of the O atom on the side group $-C_2H_4SO_3Na$ of P3TESNa is higher than that on −OH of PVA, the H atoms of the −OH groups would preferentially hydrogen-bond with the O atoms of $-C_2H_4SO_3Na$. The O atoms of the −OH groups also attract Na^+ ions electrostatically to form a bond similar

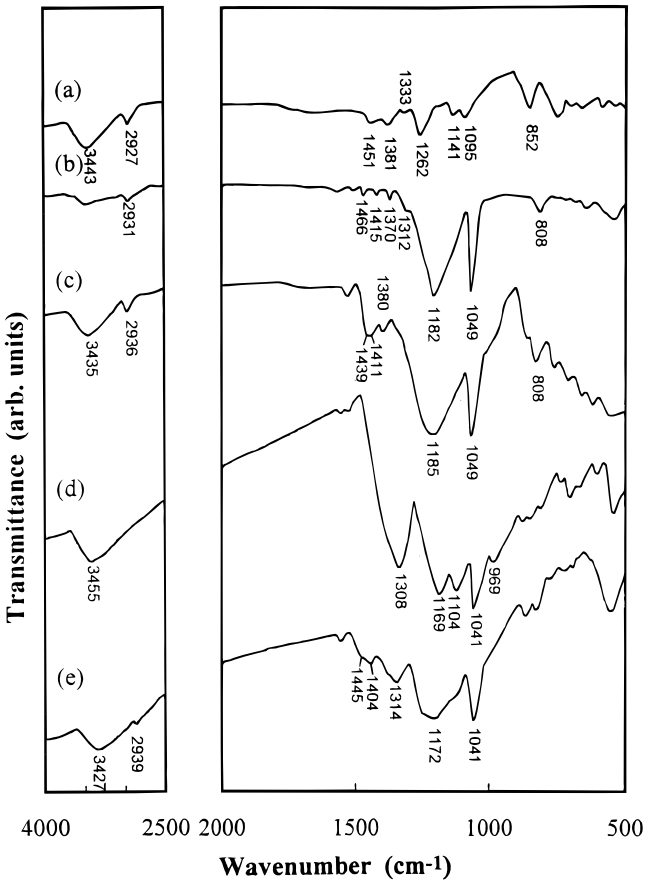

Figure 2. IR spectra of the thin films at room temperature: (a) PVA; (b) P3TESNa; (c) P3TESNa/PVA blend; (d) P3TESH; (e) P3TESH/PVA blend.

to a hydrogen bond. Both effects cause the absorption peaks due to O—H stretching and O—H bending to shift to lower wavenumbers. Also, the C—H stretching of PVA and P3TESNa shifts from 2927 and 2931 cm^{-1}, respectively, to 2936 cm^{-1} after the blending; and the absorption peak of the C—H in-plane bending on the side chain of P3TESNa shifts from 1370 to 1380 cm^{-1}, both indicating the increase of C—H bonding energy. This supports the formation of hydrogen bonding between PVA and P3TESNa, causing a decrease in the electron-pulling capability of the oxygen atom in both components and therefore an increase in the electron density of the C—H bond on the same repeat unit. Thus, complexes are expected to form between PVA and P3TESNa subchains. Such complexes could aggregate to form an amorphous region and a short-range order region, as reflected in the new diffraction peak. The disappearance of the pure PVA diffraction peak and the presence of the original P3TESNa diffraction peak (with a decrease of peak area) would indicate that a P3TESNa subchain can interact with more than one PVA subchain and parts of P3TESNa subchains have no interaction with PVA. This type of compatibility is different from that of conventional polymer blends in that the present blend has an additional phase composed of one of the two pure components.

A comparison of the spectrum of the P3TESH/PVA blend (Figure 2) with the spectra of the pure components PVA and P3TESH shows that the absorption peaks of O—H stretching and O—H bending of PVA in the blend shift from 3443 and 1451 cm^{-1} by 16 and 6 cm^{-1} to the lower wavenumbers 3427 and 1445 cm^{-1}, respectively. For P3TESH in the blend, of the four strong doping-induced vibrational modes, T_4, T_3, and T_2 shift toward higher wavenumbers and T_4 shifts from 1308 to 1314 cm^{-1}; the magnitude of the shift for T_3 and T_2 are not known, since the absorption peaks of these two T modes overlap with the stretching and bending modes of the other bondings. The absorption intensities of the three T's decrease, and that of the T_1 mode (969 cm^{-1}) decreases to become a small shoulder. The red shifts of the O—H stretching and O—H bending of PVA are due to hydrogen bonding between O atoms on the side groups $-C_2H_4SO_3H$ and $-C_2H_4SO_3-$ of P3TESH and H atoms on the side group −OH of PVA or between the proton on the side group $-C_2H_4SO_3H$ and O atoms on the -OH groups. The blue shift and decrease of absorption intensities of T_4, T_3, T_2, and T_1 indicate that partial undoping in P3TESH occurs after the blending with PVA. The presence of hydrogen bonding between P3TESH and PVA leads to formation of P3TESH/PVA complexes, similar to that in the P3TESNa/PVA blend. This is consistent with the X-ray diffraction analysis shown in Figure 1, in which the diffraction peak of disorder and short-range order phases of PVA disappear and a new diffraction peak at $2\theta = 21.2°$ is generated.

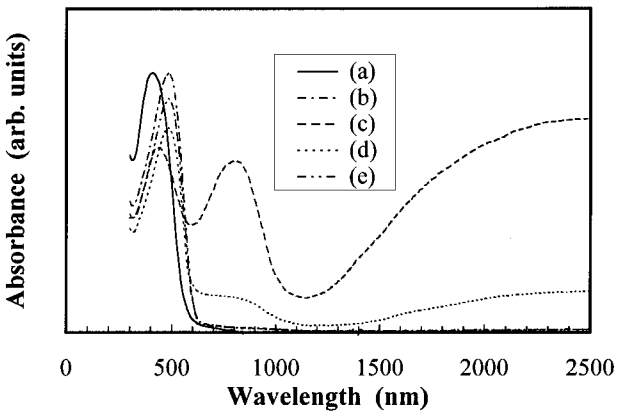

Figure 3. UV−vis−near-IR spectra of the thin films at room temperature: (a) P3TESNa; (b) P3TESNa/PVA blend; (c) P3TESH; (d) P3TESH/PVA blend; (e) P3TESNa/PVA blend after ion-exchanging.

4. Ultraviolet−Visible−Near-Infrared Spectroscopy (UV−vis−near-IR). Figure 3 shows UV−vis−near-IR spectra of P3TESNa, P3TESH, the blends of P3TESNa/PVA and P3TESH/PVA, and the treated P3TESNa/PVA blend which was obtained by exchanging the aqueous solution of P3TESNa and PVA with H^+-type ion-exchange resin for 6 h in a rotating bottle followed by casting on a glass plate and allowing to dry to give a film of thickness about 0.1−0.2 μm. For P3TESNa,[2] a comparison of spectra a and b shows that the energy of the $\pi-\pi^*$ transition decreases from 3.06 eV (406 nm, pale orange-yellow color) at the pure state to 2.58 eV (482 nm, bright orange-red color) by 0.52 eV (76 nm) after the blending with PVA; it indicates that its strong interaction with PVA leads to a considerable increase in the coplanarity of the main chains. Such a drastic change in coplanarity is equivalent to those in the thermochromism (blue shift by 74 nm, from −100 to +190 °C) of poly(3-octylthiophene)[21] and solvatochromism (red shift by 63 nm, from good solvent to poor solvent) of poly(3-hexylthiophene).[26] This is due to the strong electrostatic interaction between Na atoms and O atoms in PVA such that the P3TESNa chains become negatively charged and therefore more extended (resulting from ionic charge repulsion) as polyelectrolyte chains in water.[27] Such an effect of electrostatic interaction

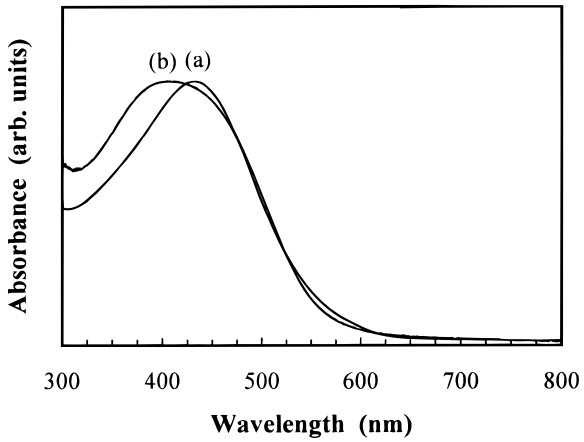

Figure 4. UV−vis−near-IR spectra of P3TESNa at room temperature: (a) aqueous solution; (b) thin film.

leading to a decrease in Na^+ ion concentration in the vicinity of P3TESNa chains is even stronger than the osmotic effect of Na^+ ions in dilute P3TESNa aqueous solution (10 mg of P3TESNa per liter of water), as can be observed from Figure 4, in which the λ_{max} (431 nm) of P3TESNa in water is longer than in the film (406 nm) by 25 nm. The red shift of P3TESNa in the aqueous solution over that in the film is opposite the blue shift by about 72 nm of poly(3-hexylthiophene) in good solvent over that in the film.[26]

Similar results are observed for the P3TESH/PVA blend. For P3TESH, a comparison of Figure 3c,d shows that the energy of the $\pi-\pi^*$ transition decreases from 2.8 eV (444 nm) in the pure state to 2.55 eV (488 nm) in the blend; and in addition, the characteristic peak intensity of polaron/bipolaron at 800 nm and the absorbance above 1150 nm decrease dramatically after the blending with PVA. The former can be attributed to the increase of coplanarity of neutral subchains of P3TESH, resulting from hydrogen bonding between the proton and O atom of PVA; such interaction causes the P3TESH subchains to become more extended as in the case of P3TESNa with PVA. The latter is due to the removal of the dopant protons from the self-doped P3TESH subchains by PVA, which decreases the self-acid-doping level. This result is consistent with the IR analysis above, which indicates the weakening and shift of the peaks of the doping-induced vibrational mode toward higher wavenumbers after blending. For the treated P3TESNa/PVA blend, no self-acid-doping is observed (Figure 3, spectrum e). This could be due to the strong interaction by hydrogen bonding between H^+ in the ion-exchange resin and PVA and between Na^+ in P3TESNa and PVA, which prevents the exchange of Na^+ and H^+.

Although P3TESNa in the aqueous solution cannot be subject to an exchange of Na^+ with H^+, P3TESNa can be doped by an addition of an external acid, such as sulfuric acid, methanesulfonic acid, and ethanesulfonic acid. To 5 mL of 0.1 mg/mL of P3TESNa/PVA aqueous solution was added 0.02 mL of the 10 N acid mentioned above. The resulting solution was spin-coated on a glass plate and allowed to dry in air and then under continuous vacuum pumping to remove the moisture. Each of the UV−vis−near-IR spectra of the resulting dry films (Figure 5) exhibits a new peak at about 800 nm and strong absorption above about 1100 nm due to the presence of polaron/bipolaron, as in the case of self-acid-doped P3TESH (Figure 3, curve c).

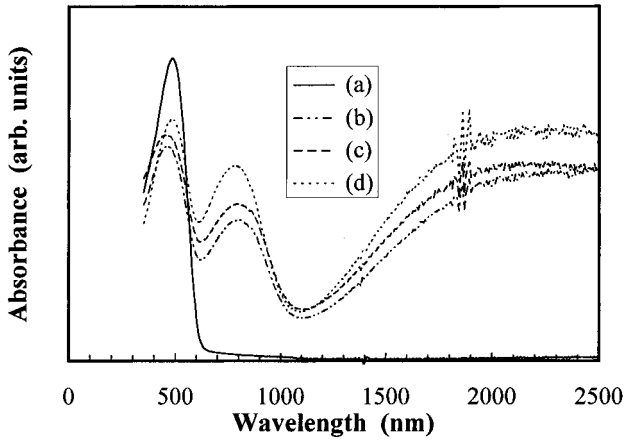

Figure 5. UV−vis−near-IR spectra of the thin films of the P3TESNa/PVA blend at room temperature before and after acid-doping: (a) before doping; (b) after $C_2H_5SO_3H$-doping; (c) after CH_3SO_3H-doping; (d) after H_2SO_4-doping.

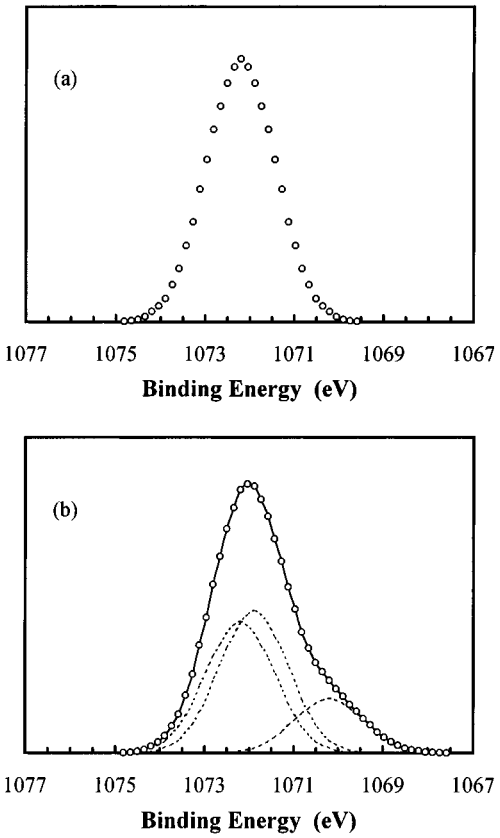

Figure 6. Na(1s) XPS core level spectra of (a) P3TESNa and (b) the P3TESNa/PVA blend. The circles are experimental results, dashed lines represent deconvolution results, and the solid line is the sum of all the dashed lines.

5. X-ray Photoelectron Spectroscopy (XPS). The Na(1s) core level spectra for the P3TESNa and P3TESNa/PVA blends are shown in Figure 6. For P3TESNa, the Na(1s) binding energy is 1072.2 eV.[28,29] For the P3TESNa/PVA blend, the Na(1s) can be deconvoluted into three components, each with a FWHM (full width at half-maximum) of 1.83 eV. The characteristic peak positions of Na(1s) are 1072.2, 1071.8, and 1070.2 eV. The first peak having the area fraction 0.4 is contributed from the P3TESNa phase, while the latter two peaks are contributed from the Na atoms in contact with the $-SO_3-$ groups which hydrogen-bond with neighboring −OH groups of PVA in the complex phase. The hydrogen bonding leads to a reduction of the interaction force

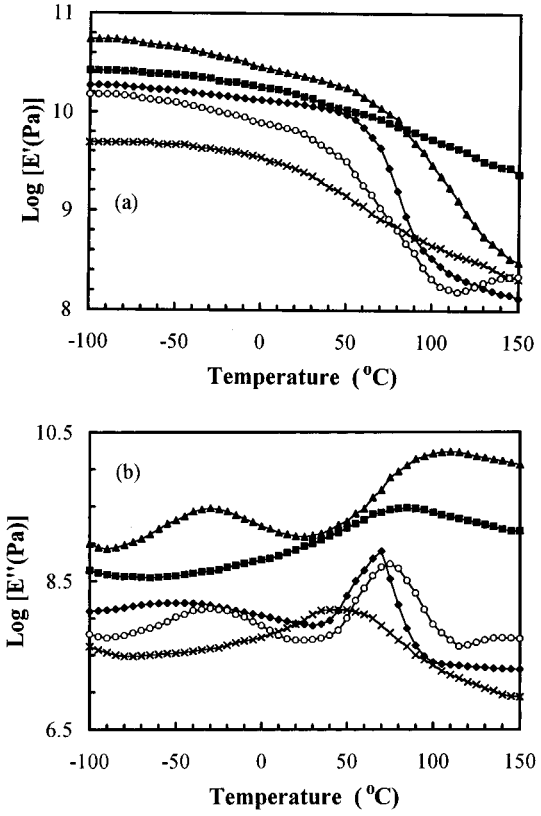

Figure 7. Dynamic mechanical analysis of PVA (◆), P3TESNa (■), P3TESH (×), and the blends P3TESNa/PVA (▲) and P3TESH/PVA (○) at the frequency 1 Hz and heating rate 2 °C/min.

Table 3. Transition Temperatures (°C) of PVA, P3TESNa, P3TESH, and the Blends P3TESNa/PVA and P3TESH/PVA from DMA

	peak temp (°C)	
sample	T_β	T_α
PVA[a]	−53	69
P3TESNa[a]		85
P3TESH[a]		46
P3TESNa/PVA blend[a,b]	−30	110
P3TESH/PVA blend[a,b]	−30	75

[a] After removal of water. [b] Mole ratio of the repeat units = 1/1.

between Na^+ and $-SO_3-$ of the $-SO_3Na$, and thus to an increase of the electron density of the Na atom, making the binding energy of Na(1s) shift to the two lower values.

6. Dynamic Mechanical Analysis (DMA). DMA for PVA, P3TESNa, P3TESH, and the blends P3TESNa/PVA and P3TESH/PVA in the temperature range −100 to +150 °C are shown in Figure 7. The characteristic temperatures T_α and T_β of the loss modulus E'' maxima are listed in Table 3. As can be seen, two transitions appear in the E'' curves of PVA[10] and the two blends, while for P3TESNa and P3TESH only one transition appears. For the transition in the higher temperature range, which is designated as an α-transition, the elastic tensile modulus E' for all the materials drops by 1−2 orders of magnitude as in the glass transition of conventional amorphous or partially crystalline polymers. Thus T_α can be regarded as T_g. The broad transition peak appears in the lower temperature range −80 to 20 °C, designated as a β-transition. For PVA, the β-transition is due to a relaxation of the hydroxyl groups[30,31] and/or local motion (crankshaft mechanism)

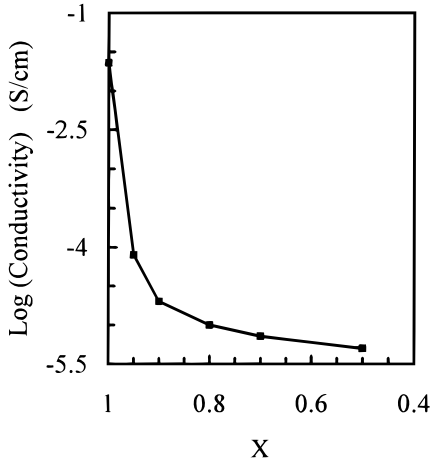

Figure 8. Conductivity of the P3TESH/PVA blend versus the mole fraction of the repeat units of PVA.

of the main chains.[32] For P3TESNa and P3TESH, no β-transition peaks are observed, indicating that the thermal motions of the short side chains are coupled with the attached thiophene rings as in the case of poly(3-butylthiophene)[12] and local motion of the main chain does not occur due to rigidity of the conjugated main chains.

For the blends of P3TESNa/PVA and P3TESH/PVA, the β-transition peaks are at −30 °C, which are higher than that of PVA (−53 °C) by 23 °C and are much sharper. The β-transition can be attributed to two types of relaxations: the first, coupled thermal motions of two bridged side chains through hydrogen bonding or electrostatic interaction (−OH groups with $-SO_3Na$ and $-SO_3H$ groups as revealed in the IR section above) and, the second, local thermal motion of the main chains of PVA as described above. Both types of relaxations should occur at a higher temperature than those of pure PVA, since the formation of bridged side chains would hinder the thermal motions of both types. Since the β peaks are significantly larger than in pure PVA, it is likely that they are contributed from the first type of relaxation. The two blends have T_α at 110 and 75 °C, much higher than those of their pure components, and the α-transitions contributed from the PVA, P3TESNa, and P3TESH phases are not observed. This is due to the presence of O···H and O···Na electrostatic interactions, which change the chain arrangement of PVA after the blending. The increase of T_α after the blending is different from that of compatible blends of two conventional polymers, which in general have T_g values located between those of the two pure components. For the P3TESH/PVA blend, the E' variation with temperature is different from the monotonic decrease in the P3TESNa/PVA blend. It decreases with increasing temperature from −100 to +105 °C and then increases with increasing temperature due to an acid-catalyzed dehydration of PVA.[10]

7. Conductivity. The logarithmic conductivity of the blends P3TESH/PVA versus mole fraction of the repeat units of PVA (x) is shown in Figure 8. The conductivity of the films first decreases rapidly with an increasing content of the PVA, from 10^{-2} S/cm of pure P3TESH film to 8×10^{-5} S/cm of the film with the mole fraction of PVA 0.05, indicating that the blending of P3TESH with PVA causes a partial undoping. As the mole fraction of PVA increases further, the conductivity of the films decreases slowly; at the mole fraction 0.5, it drops to about 5×10^{-6} S/cm. This is consistent with

the rapid decrease of the characteristic peak intensities of polaron/bipolaron in the UV−vis−near-IR spectra and the blue shift of the characteristic peaks in the IR spectra after the blending. The conductivity of the P3TESNa/PVA blend is 10^{-8} S/cm, which is lower than that of P3TESNa, 10^{-7} S/cm, by 1 order of magnitude. However, it increases from 10^{-8} to 10^{-3} S/cm after a protonic acid-doping by adding 0.02 mL of each of the 10 N sulfuric acid, methanesulfonic acid, and ethanesulfonic acid to 5 mL of the 0.1 mg of blend/mL of H_2O solution followed by film casting. The rise in conductivity after the acid-doping in conjunction with the strong UV−vis−near-IR absorption due to the formation of polaron/bipolaron indicates that the conductivity drop of P3TESH after the blending is not solely due to the dilution effect by the addition of PVA. Partial undoping of the P3TESH evidently occurs.

Conclusion

The blend of P3TESH/PVA, contains two strongly interacting components and consists of the two phases, a P3TESH phase and a P3TESH/PVA complex phase, in which no characteristic of PVA component is observed. In both phases, parts of the polymers are ordered. The complex formation is due to hydrogen bonding of the −OH with the $-SO_3H$ group or electrostatic interaction of −OH groups with H^+ doped onto the conjugated main chains accompanied with partial undoping. The P3TESH subchains that have not been self-acid-doped are red-shifted by 44 nm, resulting from an increase in coplanarity caused by a repulsion between neighboring $-SO_3-$ groups.

For the blend of P3TESNa with PVA, the strong interaction and complex formation are similar to those in the above blend. In addition, a drastic red shift by 76 nm (0.52 eV) with color changing from pale orange-yellow to bright orange-red is observed, which results from the strong electrostatic interaction between the Na^+ ion and O atom. Such a red shift is equivalent to those of the thermochromism and solvatochromism of poly(3-alkylthiophene)s.

Acknowledgment. We wish to thank the National Science Council of R.O.C. for financial aid through the projects, NSC 81-0416-E007-04 and NSC 82-0416-E-007-156.

References and Notes

(1) (a) Ikenoue, Y.; Saida, Y.; Kira, M.; Tomozawa, H.; Yashima, H.; Kobayashi, M. *J. Chem. Soc., Chem. Commun.* **1990**, 1694. (b) Ikenoue, Y.; Votani, N.; Patil, A. O.; Wudl, F.; Heeger, A. J. *Synth. Met.* **1989**, *30*, 305. (c) Patil, A. O.; Ikenoue, Y.; Basescu, N.; Colameri, N.; Chen, F.; Wudl, F.; Heeger, A. J. *Synth. Met.* **1987**, *20*, 151. (d) Arroyo-Villan, M. I.; Diaz-Quijada, G. A.; Abdou, M. S. A.; Holdcroft, S. *Macromolecules* **1995**, *28*, 975.
(2) Chen, S.-A.; Hua, M.-Y. *Macromolecules* **1993**, *26*, 7108.
(3) Chen, S.-A.; Hwang, G.-W. *J. Am. Chem. Soc.* **1994**, *116*, 7939.
(4) (a)Yue, J.; Epstein, A. J. *J. Am. Chem. Soc.* **1990**, *112*, 2800. (b) Yue, J.; Wang, Z. H.; Cromack, K. R.; Epstein, A. J.; MacDiarmid, A. G. *J. Am. Chem. Soc.* **1991**, *113*, 2665.
(5) Ikenoue, Y.; Tomozawa, H.; Saida, Y.; Kira, M.; Yashima, H. *Synth. Met.* **1991**, *40*, 333.
(6) Mizuno, F.; Kato, M.; Hayakawa, H.; Sato, K.; Hasegawa, K.; Sakitani, Y.; Saitou, N.; Murai, F.; Shiraishi, H.; Uonino, S. H. *J. Vac. Sci. Technol., B* **1994**, *12*, 3440.
(7) Hotta, S.; Rughooputh, D. D. V.; Heeger, A. J. *Synth. Met.* **1987**, *22*, 79.
(8) Inganäs O.; Gustafsson, G. *Synth. Met.,* **1990**, *37*, 195.
(9) Wang, H. L.; Toppare, L.; Fernandez, E. *Macromolecules* **1990**, *23*, 1053.
(10) Chen, S.-A.; Fang, W.-G. *Macromolecules* **1991**, *24*, 1242.
(11) Angelopoulos, M.; Patel, N.; Show, J. M. *Mater. Res. Soc. Symp. Proc.* **1994**, *328*, 173.
(12) Angelopoulos, M.; Patel, N.; Show, J. M.; Labianca, N. C.; Rishton, S. A. *J. Vac. Sci. Technol., B* **1993**, *11*, 2794.
(13) Angelopoulos, M.; Patel, N.; Saraf, R. *Synth. Met.* **1993**, *55*, 1552.
(14) Chen, S.-A.; Lee, H.-T. *Macromolecules* **1995**, *28*, 2858.
(15) Stockton, W. B.; Rubner, M. F. *Mater. Res. Soc. Symp. Proc.* **1994**, *328*, 257.
(16) Sugimoto, R.; Taketa, S.; Gu, H. B.; Yoshino, K. *Chem. Press*, **1986**, *9*, 381.
(17) Chan, H. S. O.; Ng, S. C.; Sim, W. S.; Tan, L. L.; Tan, B. T. G. *Macromolecules* **1992**, *25*, 6029.
(18) Elsenbaumer, R. L.; Shacklette, L. W. *Handbook of Conducting Polymer*; Skothein, T. A., Ed.; Marcel Dekker Inc.: New York, 1986; Vol. I, p 224.
(19) Fujii, K.; Mochizuki, T.; Imoto, S.; Ukida, J.; Matsumoto, M. *J. Polym. Sci., Part A* **1964**, *2*, 2327.
(20) Winokur, M. J.; Wamsley, P.; Moulton, J.; Smith, P.; Heeger, A. J. *Macromolecules* **1991**, *24*, 3813.
(21) Chen, S.-A.; Ni, J.-M. *Macromolecules* **1992**, *25*, 6081.
(22) *Polyvinyl Alcohol Properties and Applications*; Finch, C. A., Ed.; John Wiley & Sons Ltd., New York, 1972.
(23) Yadokoro, H. *Nature* **1948**, *161*, 929.
(24) Schaffer, H. E.; Heeger, A. J. *Solid State Commun.* **1986**, *59*, 415.
(25) Sun, Z. W.; Frank, A. J. *J. Chem. Phys.* **1991**, *94*, 4600.
(26) Inganäs O.; Salaneck, W. R.; Osterholm, J.-E.; Laakso, J. *Synth. Met.* **1988**, *22*, 395.
(27) Flory, P. J. *Principles of Polymer Chemistry*; Cornell University Press: Ithaca, NY, 1953, Chapter 14.
(28) Chastain, J., Ed. *Handbook of X-ray Photoelectron Spectroscopy*; Perkin-Elmer: Eden Prairie, MN, **1992**; p 51.
(29) Beamson, G.; Briggs, D. *High Resolution XPS of Organic Polymers*; John Wiley & Sons Ltd.: New York, 1992; p 266.
(30) Illers, K. H. *Makromol. Chem.* **1960**, *38*, 168.
(31) Kawaguchi, T. J. *Polym. Sci.* **1958**, *32*, 417.
(32) Flory, P. J. *Principles of Polymer Chemistry*; Cornell University Press: Ithaca, NY, 1953; Chapter 10.

MA951460T